Auxin-induced K⁺ channel expression represents an essential step in coleoptile growth and gravitropism

Katrin Philippar†, Ines Fuchs†, Hartwig Lüthen‡, Stefan Hoth†, Claudia S. Bauer†, Ken Haga†§, Gerhard Thiel¶, Karin Ljung‖, Göran Sandberg‖, Michael Böttger‡, Dirk Becker†, and Rainer Hedrich†**

†Julius-von-Sachs-Institut, Lehrstuhl Molekulare Pflanzenphysiologie und Biophysik, Julius-von-Sachs-Platz 2, D-97082 Würzburg, Germany; ‡Institut für Allgemeine Botanik, Universität Hamburg, Ohnhorststrasse 18, D-22609 Hamburg, Germany; §Albrecht-von-Haller Institut für Pflanzenwissenschaften, Biophysik der Pflanzen, Universität Göttingen, Untere Karspüle 2, D-37073 Göttingen, Germany; and ‖Department of Forest Genetics and Plant Physiology, Swedish University of Agricultural Sciences, SE-901 83 Umeå, Sweden

Auxin-induced growth of coleoptiles depends on the presence of potassium and is suppressed by K⁺ channel blockers. To evaluate the role of K⁺ channels in auxin-mediated growth, we isolated and functionally expressed ZMK1 and ZMK2 (*Zea mays* K⁺ channel 1 and 2), two potassium channels from maize coleoptiles. In growth experiments, the time course of auxin-induced expression of *ZMK1* coincided with the kinetics of coleoptile elongation. Upon gravistimulation of maize seedlings, *ZMK1* expression followed the gravitropic-induced auxin redistribution. K⁺ channel expression increased even before a bending of the coleoptile was observed. The transcript level of *ZMK2*, expressed in vascular tissue, was not affected by auxin. In patch-clamp studies on coleoptile protoplasts, auxin increased K⁺ channel density while leaving channel properties unaffected. Thus, we conclude that coleoptile growth depends on the transcriptional up-regulation of ZMK1, an inwardly rectifying K⁺ channel expressed in the nonvascular tissue of this organ.

To separate auxin-dependent processes related to cell division from those of cell elongation, coleoptiles represent a classical model system for studies on the regulation of cell growth and tropisms. In this tissue the number of cells remains constant and auxin coming from the tip induces rapid cell elongation. Coleoptile segments lacking auxin-producing zones grow only under growth hormone supplementation. During cell elongation, cell surface area increases and cell wall polysaccharides, cell wall proteins, and plasma membrane components are secreted. Genes responding to changes in auxin concentration, as the H⁺-ATPase (1–3) or the SAURs (small auxin up RNAs) and Aux/IAA (auxin/indole-3-acetic acid) genes, have been shown to accompany cell elongation (4, 5). Apart from the H⁺-ATPase, none of the auxin-induced genes known so far are involved with events at the plasma membrane (6). The bending of coleoptiles, resulting from gravitropic stimulation, was postulated by Cholodny and Went (7) to result from an asymmetrical distribution of growth hormones. This hypothesis was confirmed by Iino (8) and Parker and Briggs (9).

In well abraded coleoptiles, however, it has been shown recently that auxin-induced growth strictly depends on external K⁺ supply (10). Because Rb⁺ could partially replace K⁺ in this process, but neither Na⁺ nor Li⁺, and the plant K⁺ channel blockers TEA⁺ (tetraethylammonium), Ba²⁺, and Ca²⁺ suppressed auxin-induced growth, K⁺-uptake channels seem to play a crucial role in auxin action.

Because in earlier studies we could show that the plasma membrane of corn coleoptile cells is equipped with a voltage-dependent, inwardly rectifying K⁺ channel (11, 12), we now isolated *ZMK1* and *ZMK2* cDNAs coding for coleoptile K⁺ channels. To understand their role in auxin-dependent signal transduction, we examined the expression pattern of *ZMK1* and *ZMK2* and functionally expressed these ion channels in *Xenopus* oocytes. Using the patch-clamp technique, we followed the increase in channel density in coleoptile cells stimulated by auxin. Molecular studies on the expression of *ZMK1*, auxin-induced growth, and gravitropism displayed similar kinetics.

Thus, we could provide evidence that coleoptile elongation and bending involves a transcriptional up-regulation of inwardly rectifying K⁺ channels.

Materials and Methods

Maize Strains and Growth Conditions. Cloning and Northern blot experiments were performed on tissues from *Zea mays* seedlings (hybrid corn cv. "Apache," "Garant"). Maize caryopses were soaked in water, germinated on moistened filter paper in darkness, and grown further under red light ($0.2 \ \mu\text{mol}\cdot\text{m}^{-2}\cdot\text{s}^{-1}$) at 25°C. For gravitropic stimulation, seedlings grown in 1% agar were displaced by 90°. The plane passing through the two vascular bundles of the coleoptile was parallel to the direction of gravity. Coleoptiles were harvested with a ≤2.5-cm length, lacking the apical 3 mm of the tip region.

Cloning of *ZMK1* and *ZMK2* cDNA. Degenerated oligonucleotide primers, directed toward homologous regions of known plant K⁺ channels, were used to amplify a corresponding region from reverse-transcribed maize seedling RNA. Using the Marathon cDNA synthesis kit (CLONTECH) in combination with gene-specific primers, we amplified overlapping N- and C-terminal K⁺ channel fragments. The corresponding full-length clones were generated in a single PCR step by using primers flanking the 5′ and 3′ ends of the coding sequences and ligated into pZErO-1 vector (Invitrogen).

Northern Blot Analysis. Total RNA was isolated from maize seedlings by using the Plant RNeasy Extraction kit (Qiagen) followed by purification of poly(A)⁺ RNA with Dynabeads (Dynal). For quantification of transcript abundance, dotted poly(A)⁺ RNA was hybridized at 68°C in P_i buffer (250 mM NaP_i/pH 7.2/7% SDS/1 mM EDTA/1% BSA) against ³²P-radiolabeled, full-length cDNA probes of *ZMK1* and *ZMK2*. In parallel, poly(A)⁺ RNA dots were hybridized at 42°C against a [γ-³²P]dATP end-labeled oligo(dT) probe, modified according to ref. 13. The relative transcript content was calculated by normalizing the signal density of the specific channel probe to that of the oligo(dT) probe (mean of 5, 10, and 15 ng of dotted mRNA).

Two-Electrode Voltage-Clamp Experiments. *In vitro* transcription of cRNA as well as preparation and injection of oocytes were carried out as described in ref. 14. Two-electrode voltage-clamp measurements of ZMK1 and ZMK2 channels and data analysis were performed as described previously (14–16). The standard external solution for ZMK1 contained 100 mM KCl, 1 mM $CaCl_2$, 2 mM $MgCl_2$, and 10 mM Mes/Tris (pH 5.6) and, for ZMK2, 50 KCl, 2 $MgCl_2$, 10 Mes/Tris (pH 7.2). In pH-step experiments pH 7.4 was buffered with 10 mM Mes/Tris, and pH 4.5 was buffered with citrate/Tris. The Rb^+ conductance was studied in 100 mM RbCl, compared with 100 mM KCl at a membrane voltage of −150 mV.

Patch-Clamp Experiments. Patch-clamp experiments in the whole-cell and cell-attached mode were performed as described in refs. 17 and 18 on cortical and epidermal coleoptile protoplasts, which were isolated according to refs. 12 and 19. Current densities were calculated from the steady-state current at −140 mV. The standard bath and pipette solution contained 30 mM KGluc, 20 mM $CaCl_2$, 1 mM $MgCl_2$, and 10 mM Mes/Tris (pH 5.6) and 150 mM KGluc, 2 mM $MgCl_2$, 10 mM EGTA, 2 mM MgATP, and 10 mM Hepes/Tris (pH 7.2), respectively. To study the Rb^+ conductance, 30 mM KGluc in the bath was replaced by 30 mM RbCl. Protoplasts for cell-attached measurements were incubated in standard bath solution containing 500 mM sorbitol, 1 mM $CaCl_2$, 60 mM Mes/KOH (pH 6.1), giving a K^+ concentration of 30 mM. The standard pipette solution contained 120 mM KCl and 20 mM Mes/KOH (pH 6.1). In cell-attached recordings the free-running membrane voltage is unknown, and, therefore, the relative voltage (V′) is given as the negative command voltage of the clamp circuit. In our measuring conditions, the free-running voltage of the protoplasts can be assumed to be about −20 mV so that the test voltage, V*, is about 50 mV more negative than V′. For individual combinations of solutions, liquid junction potentials were estimated according to Neher (20), and voltages were corrected accordingly. For voltage-ramp protocols, the patch first was clamped from holding V* (= −90 to −110 mV) to conditioning voltage (700 ms at +75 or +100 mV) to inactivate the K^+-inward rectifier. The patch then was subjected to voltage ramps (32–47 mV·s⁻¹) from the conditioning voltage to −200 mV ≤ V* ≤−125 mV.

Growth Experiments. Auxin-induced growth of SiC-abraded coleoptile segments was monitored as described (10). For Northern blot experiments, 30–40 coleoptile segments were removed from the buffer and subjected to RNA preparation at indicated times. 2-NAA (1-naphtalene-acetic acid), fusicoccin (FC), acidification, and IAA dose-response experiments as well as cycloheximide (CHX) treatments were performed with nonabraded coleoptile segments, incubated for 60 min with the respective effector.

Analysis of Endogenous IAA Concentrations. Coleoptiles of 2-cm length were selected and harvested after gravitropic stimulation. After cutting the coleoptile in upper and lower halves, the segments were sectioned further into four 5-mm parts. Tissue from three individual seedlings were pooled and weighed for each analysis (10- to 20-mg tissue/sample). After harvesting, the tissue was frozen immediately in liquid nitrogen. Purification and quantification of endogenous concentrations of IAA were done on triplicate samples by GC-MS as described (21). The mass spectrometer was operated in the selected-reaction mode (SRM), and the IAA concentration in the sample was calculated from isotopic dilution of 500 pg of ¹³C6-labeled IAA added as internal standard before purification.

Results and Discussion

Isolation, Characterization, and Localization of *ZMK1* and *ZMK2* cDNA. We isolated *ZMK1* and *ZMK2* from maize seedling cDNA via reverse transcription–PCR and rapid amplification of cDNA ends techniques. The cloning strategy took advantage of highly conserved regions in the *Shaker*-related, but inwardly rectifying family of known plant K^+-uptake channels. Identification and sequence analysis of the *ZMK1* (2,661 bp, GenBank accession no. Y07632) and *ZMK2* (2,547 bp, GenBank accession no. AJ132686) cDNAs revealed the basic features of this family. On the amino acid level, ZMK1 showed the highest homology (61% identity) to the *Arabidopsis* root K^+ channel AKT1 (22) and, therefore, belongs to this plant K^+ channel subfamily. Based on a 56% amino acid identity, ZMK2 is closely related to the phloem K^+ channel AKT3 (23, 24). From hydrophobicity analysis of both channels we deduced six putative transmembrane domains (S1–S6) with a proposed voltage sensor in segment 4 and a K^+-selective pore (P) formed by the amphiphilic linker between S5 and S6 (for structure–function analysis of plant K^+ channels, see ref. 25). In Northern blot analysis of coleoptile tissue we identified *ZMK1* as a 2.8-kb and *ZMK2* as a 2.7-kb transcript, respectively (Fig. 1*A*). To determine the distribution of *ZMK1* and *ZMK2* within the coleoptile, we separated non-vascular from vascular-enriched tissue. Whereas *ZMK1* is expressed in both tissues, *ZMK2* transcripts were preferentially expressed in the fraction containing vascular bundles (Fig. 1 *A* and *B*). We could, however, not exclude that the *ZMK1* signal in vascular-enriched tissue is due to at least 50% contamination by nonvascular cells (see Fig. 1*A Right*). In 4-day-old maize seedlings the expression of both channels could be detected in rapid-growing coleoptiles and mesocotyls, whereas *ZMK2* mRNA also was found in developing and strongly vasculated primary leafs (Fig. 1*C*). It should be mentioned that *ZMK2* homologues from *Arabidopsis thaliana* and *Vicia faba* are expressed predominantly in vascular tissues, too (24).

Functional Analysis of ZMK1 and ZMK2. When expressed in *Xenopus* oocytes the gene product of *ZMK1* showed the characteristic properties of a voltage-dependent, inwardly rectifying plant K^+-uptake channel (Fig. 2 *Left*). Therefore, ZMK1 represents the first member of the AKT1-type K^+ channel subfamily functionally expressed in *Xenopus* oocytes (26). In two-electrode voltage-clamp experiments, ZMK1 activated on hyperpolarization to membrane potentials negative to −90 mV (Fig. 2*C Left*). In contrast to ZMK1, the gene product of *ZMK2* in *Xenopus* oocytes activated in an almost voltage-independent fashion with fast kinetics (Fig. 2 *Right*). In agreement with K^+-selective channels, K^+ currents through ZMK1 and ZMK2 increased as a function of the external K^+ activity. The current reversal potential followed the Nernst potential with a shift of 56.3 mV for ZMK1 ($n = 4$ in 10 mM K^+; $n = 9$ in 100 mM K^+) and 59.4 mV for ZMK2 ($n = 3$) per 10-fold change in external K^+ activity. In contrast to potassium, both K^+ channels did not conduct sodium ions (not shown). In the maize cultivar used for cloning both K^+ channels, protoplasts from coleoptile cortex and ZMK1-expressing oocytes in Rb^+ solutions conducted only $6.9 \pm 0.8\%$ ($n = 6$) and $17.8 \pm 1.7\%$ ($n = 3$) of the current observed with K^+. In tight correlation with the suppression of auxin-dependent coleoptile elongation by Cs^+ (see below) and the inhibition of K^+-uptake channels in coleoptile protoplasts (11), ZMK1 was blocked by millimolar Cs^+ concentrations in a voltage-dependent manner. A voltage-independent block was mediated by TEA^+, which also inhibits auxin-induced coleoptile elongation and K^+ uptake into coleoptile protoplasts (10, 12). ZMK2 exhibits a Cs^+ and TEA^+ dependence similar to ZMK1 (data not shown). Upon a drop in extracellular pH from 7.4 to 5.6, K^+ currents through ZMK1 and the inward rectifier in coleoptile
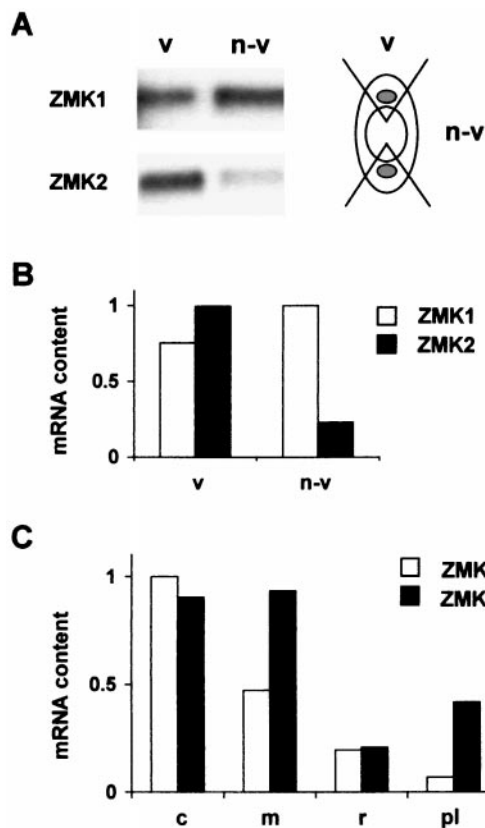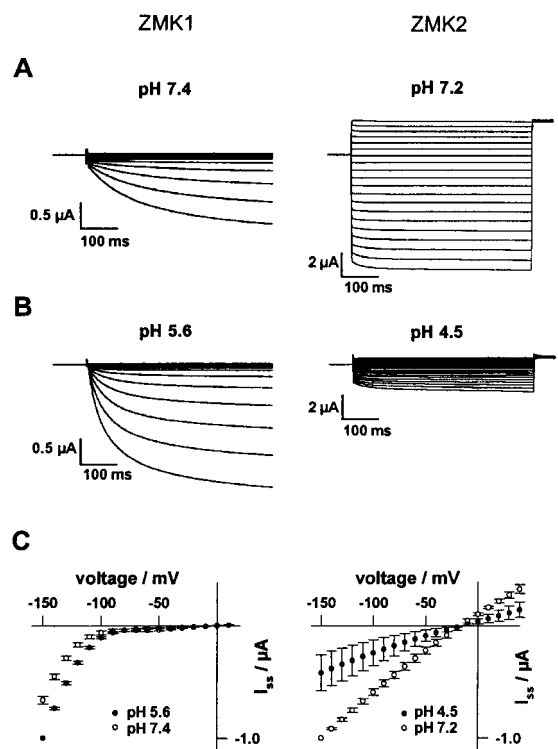
Fig. 1. Expression pattern of *ZMK1* and *ZMK2* in maize seedlings. (*A Left*) Northern blot of 1 μg of mRNA from vascular-enriched (v) and nonvascular (n-v) coleoptile tissues, hybridized against a radiolabeled *ZMK1* and *ZMK2* cDNA probe. (*Right*) Scheme of a coleoptile cross-section to illustrate the fragmentation into vascular and nonvascular parts. Notice that vascular-enriched parts contain nonvascular tissue. (*B*) Relative quantification of *ZMK1* and *ZMK2* mRNA content in vascular (v) and nonvascular (n-v) coleoptile tissues. Relative mRNA content of *ZMK1* (open bars) and *ZMK2* (solid bars) was calculated by normalizing *ZMK1* and *ZMK2* signal density from *A* as described in *Materials and Methods*. The transcript content of *ZMK2* in vascular tissue was set to 1.0 (arbitrary units). (*C*) Relative content of *ZMK1* and *ZMK2* mRNA in seedling tissues. The transcript content, representative of $n = 3$ experiments, was quantified from the signal density of mRNA dot blots as described. The mRNA content of *ZMK1* in coleoptiles was set to 1.0 (arbitrary units). c, coleoptile; m, mesocotyl; r, root; pl, primary leaf.


Fig. 2. Voltage dependence and pH sensitivity of *ZMK1* and *ZMK2* expressed in *Xenopus* oocytes. (*A Left*) Inward currents of ZMK1 were elicited in response to 500-ms voltage pulses from +10 mV to −150 mV (10-mV decrements) from a holding potential of −20 mV. (*Right*) From the zero current potential of ZMK2, 500-ms pulses from +40 mV to −150 mV were applied in 10-mV decrements. (*B Left*) Upon acidification of the extracellular solution from pH 7.4 to 5.6, ZMK1 currents increased. (*Right*) Upon acidification from pH 7.2 to 4.5, ZMK2 currents decreased. (*C*) Steady-state currents (I_{ss}) at the end of the voltage pulses from *A* (○) and *B* (●) were normalized to I_{ss} (−150 mV) and plotted against the membrane voltage as mean ± SE ($n = 4$).

cells reversibly increased (Fig. 2 *Left*; data not shown), indicating that *in vivo* ZMK1 is capable of responding to apoplastic acidification. An opposite pH dependence was observed with ZMK2 (Fig. 2 *Right*). In line with the predominant expression of ZMK2 in the vascular tissue (Fig. 1), we never observed ZMK2-like currents in coleoptile protoplasts derived from cortex and epidermis cells used in this study.

Regarding the expression pattern and the biophysical characteristics, such as permeation properties, voltage dependence, interaction with blocking ions, and acid activation, of the coleoptile K$^+$ channels *in vivo* and *in vitro* (for expression system-dependent variations, see ref. 27), we conclude that ZMK1 represents the major inward rectifier in cortex and epidermal cells of growing coleoptiles.

Active Auxins Induce K$^+$ Channel Expression. In coleoptile segments auxin evokes growth under ionic conditions that resemble the selectivity range of inwardly rectifying K$^+$ channels (K$^+$ > Rb$^+$ ≫ Li$^+$, Na$^+$). Furthermore, coleoptile growth can be blocked by the K$^+$ channel blockers TEA$^+$ and divalent cations (10).

Additional studies on the growth inhibition by the channel blocker Cs$^+$ revealed that auxin-induced coleoptile growth was blocked at concentrations ≥1 mM (not shown), in line with the Cs$^+$ block of the K$^+$-uptake channel in coleoptile protoplasts (11) and ZMK1 in *Xenopus* oocytes.

To define the physiological significance of *ZMK1* and *ZMK2* in cell elongation, we measured the growth rates of corn coleoptiles after stimulation by the auxin 1-NAA. Using "auxa-nometers," we were able simultaneously to monitor the elongation rates of corn coleoptile segments (10) and isolate mRNA at given time intervals. Fig. 3*A* shows that the elongation of coleoptiles is delayed by about 15 min with respect to the onset of auxin treatment. The peak growth rate of the initial auxin response was reached about 45 min after stimulus onset. This peak was followed by sustained growth after 60 min. The level of *ZMK1* expression followed this growth rate pattern (Fig. 3*B*). The *ZMK1* transcript levels increased significantly after 45 min of auxin treatment, reaching a maximum at 60–75 min ($n = 3$). In the absence of auxin, growth rates and *ZMK1* expression were low throughout the time course of the experiment (Fig. 3 *A* and *B*). The induction of *ZMK1* transcription depended on the concentration of the physiological-active auxin IAA, characterized by a saturation type of behavior with a K_M of around 0.1 μM IAA (Fig. 3*C*). ZMK2, expressed in the vascular tissue of maize coleoptiles, in all experiments, however, lacked transcriptional activation by auxin (not shown).

Growth experiments have shown that auxin action is ac-
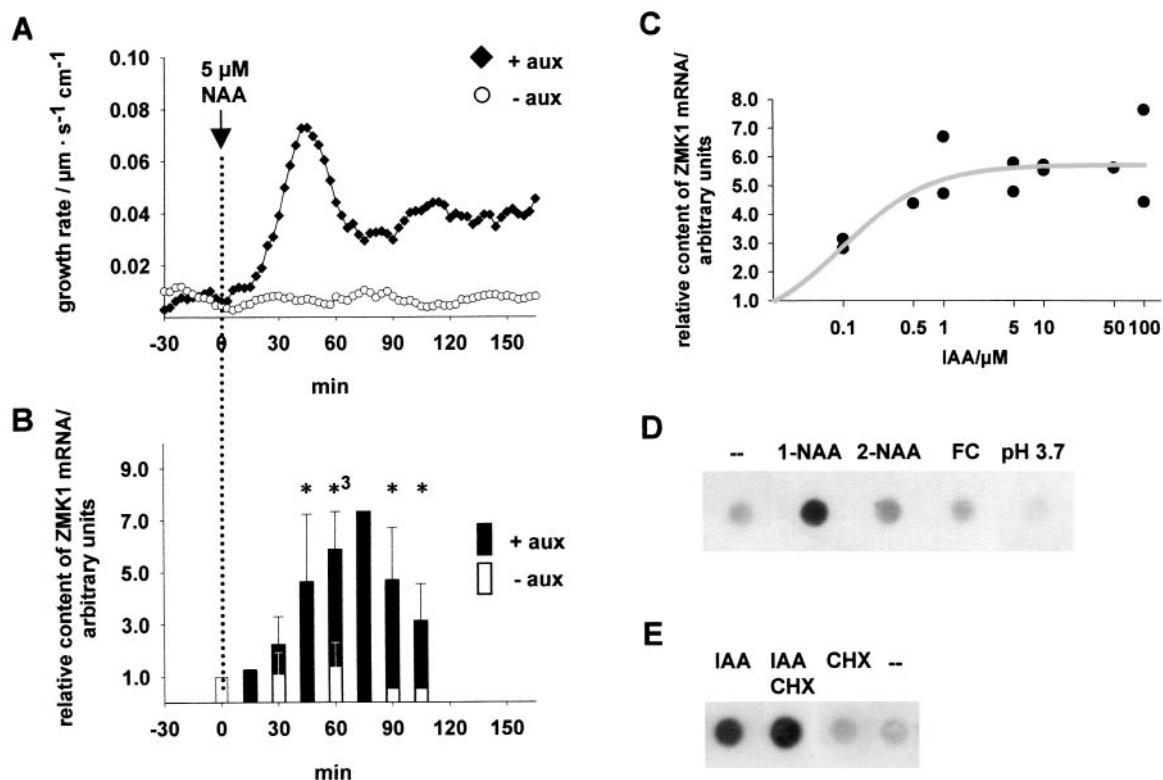
Fig. 3. Characterization of the transcriptional induction of *ZMK1* by auxin. (*A*) Kinetics of auxin-induced coleoptile growth. Representative growth curves of abraded coleoptile segments in K^+-containing medium in the presence and absence of 5 μM NAA (◆ and ○, respectively). (*B*) Kinetics of auxin-induced *ZMK1* expression. Transcript abundance of *ZMK1* in coleoptile segments in the presence and absence of 5 μM NAA (solid and open bars, respectively). The content of *ZMK1* mRNA at the given times [*n* = 3, 75 min (■); *n* = 1, 90 and 105 min □)] was analyzed by Northern dot blots and quantified as described in *Materials and Methods*. The transcript contents were normalized to the *ZMK1* mRNA level at *t* = 0 min, which was set to 1.0 (arbitrary units). According to a *t* test the *ZMK1* mRNA content in auxin-treated coleoptiles was significantly different from untreated tissue after 45 min (5% level). The statistical significance is indicated by asterisks (∗, 5% level; ∗³, 0.1% level). (*C*) Concentration dependence of the auxin-induced *ZMK1* expression. Half-logarithmic plot of *ZMK1* mRNA content (●) in coleoptile segments after 60 min of incubation with different IAA concentrations (*n* = 2). The relative content of *ZMK1* mRNA was analyzed as described, and the background level of *ZMK1* mRNA (0 μM IAA) was set to 1.0 (arbitrary units). The concentration dependence of *ZMK1* expression can be fitted with a saturation function (gray line), characterized by a K_M of about 0.1 μM IAA. (*D*) *ZMK1* transcription is induced specifically by the active auxin 1-NAA. Shown are Northern dot blots of 0.5 μg mRNA from nontreated (–) coleoptiles and tissues treated for 60 min with 5 μM 1-NAA, 5 μM 2-NAA, and 1 μM FC and incubated in pH 3.7, which were hybridized against a radiolabeled *ZMK1* probe. (*E*) Auxin-induced transcription of *ZMK1* is cycloheximide-independent. Shown are Northern dot blots of 0.5 μg mRNA from coleoptiles treated for 60 min with 5 μM IAA (IAA), 5 μM IAA, 70 μM CHX (IAA CHX), and 70 μM CHX (CHX) and nontreated tissue (–), which were hybridized against a radiolabeled *ZMK1* probe.

companied by extracellular acidification (10). To prove whether the increase in *ZMK1* expression is directly dependent on auxin or is a consequence of pH changes, we followed *ZMK1* transcript levels in response to 1-NAA, 2-NAA, the fungal toxin FC, and protons. Fig. 3*D* demonstrates that the induction of *ZMK1* transcription is restricted to the active auxin 1-NAA and could not be initiated by 2-NAA, FC, or extracellular acidification. This indicates that *ZMK1* expression is under the control of the auxin-signaling pathway. Treatment with the protein-synthesis inhibitor CHX did not prevent the auxin-dependent increase in *ZMK1* transcripts (Fig. 3*E*). This channel gene therefore may be classified as an early auxin-response gene (28).

Auxin Increases K^+ Channel Density. Because in previous whole-cell patch-clamp studies auxin did not alter the properties of K^+ uptake channels in coleoptile protoplasts (11, 12), we monitored the anticipated changes in channel density in the cell-attached configuration. In this mode, which maintains the integrity of the cytoplasm, auxin increased the density of the inward rectifier in a time-dependent manner (Fig. 4). In the absence of NAA in the bath medium, only background currents were observed. After challenging cells with 10 μM

1-NAA and hyperpolarized voltages, the inward current increased after a lag phase of >10 min (Fig. 4). Biophysical analysis of the K^+ currents, which rose nearly two-fold after 15 and 30 min (Fig. 4*B*), revealed that the current activation is neither due to a hyperpolarization of the free-running membrane potential nor to a kinetic modulation of channel gating (not shown). Thus, the most likely explanation is an increase in the number of active channels in the plasma membrane, which seems to result from a signal-transduction pathway leading to the fusion of newly synthesized K^+ channels into the membrane patch.

To underline this hypothesis, we investigated the K^+ current densities of protoplasts derived from auxin-pretreated and -depleted coleoptile segments in the whole-cell configuration. The median of current densities in coleoptile plasma membranes (8.7 μA/cm², *n* = 38) increased 3-fold (significant on a 5% and 1% error level according to a Mann–Whitney test) when treated with 5 μM (23.6 μA/cm², *n* = 24) or 10 μM 1-NAA (27.5 μA/cm², *n* = 18) for 3 hr. The auxin-evoked increase in K^+ channel densities in the short term and its maintenance during sustained growth therefore is in agreement with the long-term coleoptile growth rates and the change in *ZMK1* transcript levels shown in Fig. 3.
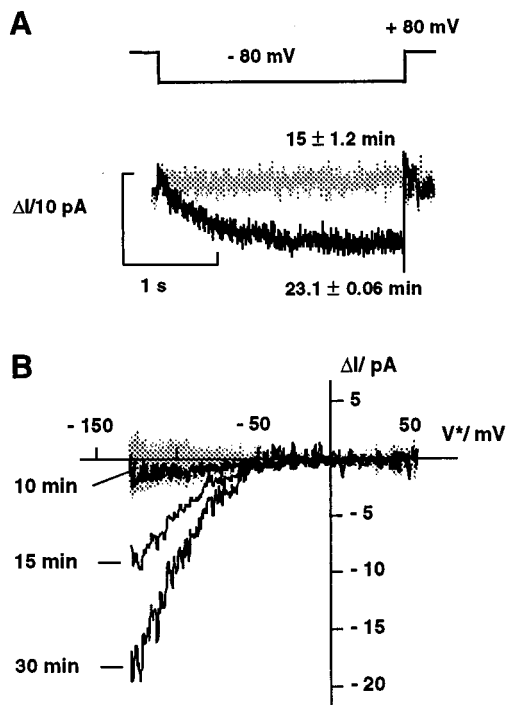
Fig. 4. Auxin-induced increase in K$^+$ channel density in coleoptile protoplasts. (*A*) In the cell-attached mode, K$^+$ currents increased after the addition of 10 μM 1-NAA after a voltage step from +80 mV to −80 mV. Auxin-evoked currents (ΔI) were obtained by subtracting the mean current response (I$_m$) over 7 min before the addition of auxin (*n* = 12) from I$_m$ collected 15 min (gray trace, *n* = 6) and 23 min (black trace, *n* = 8) after auxin treatment. With incubation times ≥23 min, auxin induces a time-dependent inward conductance. (*B*) Development of the K$^+$-inward conductance in response to 10 μM 1-NAA. In the presence of auxin, repetitive voltage ramps (*n* = 14) monitor the increase in K$^+$ current at times ≥15 min. In the absence of auxin only background currents were recorded (shaded area). Each trace in *A* and *B* represents the mean of *n* voltage ramps averaged.

ZMK1 **Expression Follows Auxin Redistribution During Gravitropism.** To explore the importance of auxin-regulated *ZMK1* expression during physiological processes in intact plants, we determined the distribution of IAA as well as *ZMK1* and *ZMK2* mRNAs during the gravitropic bending of coleoptiles. After displacement of intact maize seedlings into a horizontal position (90° angle, Fig. 5*A*), endogenous IAA concentration was measured in 5-mm coleoptile segments from the apical part and downward to the mesocotyl. Each segment was divided into an upper and lower half to investigate the redistribution of IAA. Interestingly, after only 5 min of gravitropic stimulation, a significant increase in the levels of free IAA was observed and was most pronounced in the apical parts of the coleoptile (Fig. 5*B*). After 15 min, a redistribution of IAA occurred in the coleoptile tip with a 25% difference between the upper and the lower side. The redistribution thereafter succeeded down the coleoptile, reaching significant differences between all upper and lower segments after 45 min of stimulation (Figs. 5*B* and 6*A*). The largest difference in IAA concentration between lower and upper halves is found in the segment 0.5–1 cm below the tip (Fig. 5*B*). In this segment after 45 min, a significant reduction of IAA in the upper part of the coleoptile was detected. The endogenous IAA concentrations in the coleoptile vary between 0.2 and 0.08 μM (tip/base). This concentration range represents the slope of the dose–response curve for the IAA-induced *ZMK1* transcription (Fig. 3*C*).

After 30 min of gravistimulation the *ZMK1* transcripts in the
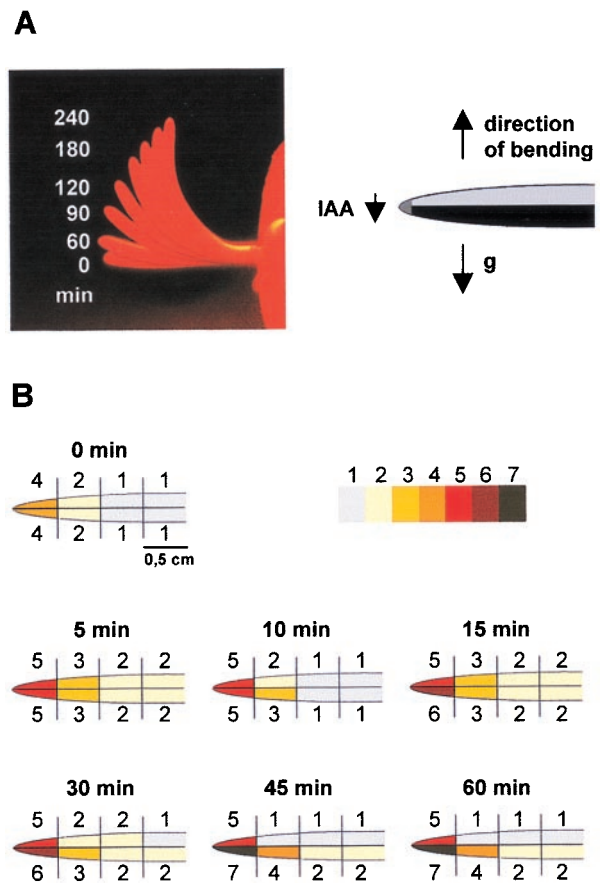
Fig. 5. Coleoptile bending and redistribution of endogenous IAA concentration in response to gravistimulation. (*A Left*) Time-dependent coleoptile bending (0–240 min) in response to a 90° gravistimulation. (*Right*) Cartoon of a gravistimulated coleoptile. (*B*) IAA concentration (pg IAA/mg fresh weight, mean of *n* = 3 experiments) in 0.5-cm segments of coleoptile halves, gravistimulated for 0, 5, 10, 15, 30, 45, and 60 min. The IAA spectrum was decomposed into seven concentration ranges and highlighted by a color code. **1,** 10.8–13.9 ± 3.0; **2,** 14.1–17.9 ± 3.3; **3,** 19.9–23.5 ± 5.5; **4,** 16.9–31.2 ± 5.9; **5,** 34.6–42.5 ± 7.6; **6,** 48.7–49.4 ± 6.5; **7,** 51.1–58.8 ± 8.0 pg IAA/mg fresh weight.

upper side, which is growth-restricted and auxin-depleted (8), decreased in a time-dependent manner, resulting in background signals after 90 min (Fig. 6*B*). In the lower half, which is characterized by elevated IAA levels and enhanced growth, the *ZMK1* mRNA level increased slightly during the experiment. This differential expression of the *ZMK1* gene within the coleoptile was detectable even before the first bending could be observed (Fig. 5*A* and ref. 29). The kinetics of the transcriptional induction of *ZMK1* in gravistimulated maize seedlings correlated with those of the *ZMK1* mRNA increase during auxin-induced cell elongation (Fig. 3*B*) and are in line with the rates of IAA redistribution, determined in gravistimulated coleoptiles (Figs. 5*B* and 6*A* and ref. 8). The content of *ZMK2* mRNA in the coleoptile halves, however, remained constant throughout the initiation of gravitropic bending (not shown).

Conclusions. Coleoptile elongation in response to auxin is characterized by a biphasic process (30). A transient increase in growth, initiated 15 min after stimulus onset, is superimposed by saturation-type growth kinetics. This second phase, biochemically distinct from the first response, has been associated with long-term, steady-state growth. Both phases are accompanied by increased proton extrusion into the apoplast (10). Although
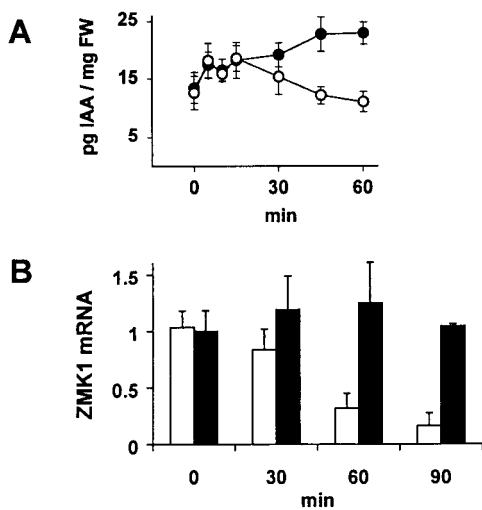
Fig. 6. Kinetics of IAA redistribution and differential *ZMK1* expression during gravistimulation of coleoptiles. (*A*) Time-dependent IAA redistribution in upper (○) and lower (●) coleoptile halves after gravistimulation. The figure shows the IAA concentration per mg fresh weight (FW, $n = 3 \pm$ SE) in segments 0.5–1.5 cm behind the tip (compare with Fig. 5*B*). (*B*) Relative transcript content of *ZMK1* in upper (open bars) and lower (solid bars) coleoptile halves 0.5–1.5 cm behind the tip after 0, 30, 60, and 90 min of gravistimulation. The mRNA content ($n = 3 \pm$ SE) was quantified as described in *Materials and Methods*. The level of *ZMK1* mRNA in the upper half at $t = 0$ min was set to 1.0 (arbitrary units).

auxin neither directly modulated the properties of K^+-uptake channels in coleoptile protoplasts (11, 12) nor the features of the

ZMK1 gene product when expressed in *Xenopus* oocytes (unpublished data), acidification resulted in an immediate increase in channel activity (Fig. 2). Thus, we might conclude that the initial growth response involves posttranslational, auxin-dependent up-regulation of the H^+-ATPase (1, 2) and, in turn, voltage as well as acid activation of K^+-uptake channels (Fig. 2 and ref. 31). In contrast to the first phase of auxin action, further cell elongation in the second phase, represented by sustained growth rates, seems to require the induction of gene expression. Hence, this leads to the incorporation of additionally synthesized K^+ channels into the plasma membrane of the elongating cell and, finally, increases the number of channels in the membrane (Fig. 4).

The experiments with intact maize seedlings indicate that the initial sensing of gravitropism probably causes a very rapid release of free IAA from conjugated IAA pools. The decrease in IAA in the upper segments after 30 min then is due to the redistribution of free IAA in the coleoptile tip, most likely by altering the transport capacity (32–35) on the upper and lower sides. The differential expression of *ZMK1* between the upper and lower halves of gravistimulated coleoptiles is in line with the spatial and temporal pattern of an auxin redistribution (Fig. 5 and ref. 8). We therefore suppose that in intact coleoptiles, transcriptional regulation of *ZMK1* represents a key step in response to physiological growth stimuli. The transcript level of *ZMK1* in elongating coleoptiles increased 5- to 7-fold, and the number of channel proteins per cell increased about 3-fold. Therefore, the auxin-induced increase in channel number during cell expansion seems to present a mechanism to maintain K^+ accumulation and turgor.

1. Felle, H., Peters, W. & Palme, K. (1991) *Biochim. Biophys. Acta* **1064,** 199–204.
2. Lohse, G. & Hedrich, R. (1992) *Planta* **188,** 206–214.
3. Hager, A., Debus, G., Edel, H. G., Stransky, H. & Serrano, R. (1991) *Planta* **185,** 527–537.
4. McClure, B. A. & Guilfoyle, T. (1989) *Science* **243,** 91–93.
5. Abel, S., Oeller, P. W. & Theologis, A. (1994) *Proc. Natl. Acad. Sci. USA* **91,** 326–330.
6. Sitbon, F. & Perrot-Rechenmann, C. (1997) *Physiol. Plant.* **100,** 443–455.
7. Went, F. W. & Thimann, K. V. (1937) *Phytohormones* (Macmillan, New York).
8. Iino, M. (1991) *Plant Cell Environ.* **14,** 279–286.
9. Parker, K. E. & Briggs, W. R. (1990) *Plant Physiol.* **94,** 1763–1769.
10. Claussen, M., Lüthen, H., Blatt, M. & Böttger, M. (1997) *Planta* **201,** 227–234.
11. Hedrich, R., Bregante, M., Dreyer, I. & Gambale, F. (1995) *Planta* **197,** 193–199.
12. Thiel, G., Brüdern, A. & Gradmann, D. (1996) *J. Membr. Biol.* **149,** 9–20.
13. Hollander, M. C. & Fornace, A. J. J. (1990) *BioTechniques* **9,** 174–179.
14. Müller-Röber, B., Ellenberg, J., Provart, N., Willmitzer, L., Busch, H., Becker, D., Dietrich, P., Hoth, S. & Hedrich, R. (1995) *EMBO J.* **14,** 2409–2416.
15. Hedrich, R., Moran, O., Conti, F., Busch, H., Becker, D., Gambale, F., Dreyer, I., Kuech, A., Neuwinger, K. & Palme, K. (1995) *Eur. Biophys. J.* **24,** 107–115.
16. Becker, D., Dreyer, I., Hoth, S., Reid, J. D., Busch, H., Lehnen, M., Palme, K. & Hedrich, R. (1996) *Proc. Natl. Acad. Sci. USA* **93,** 8123–8128.
17. Schulz-Lessdorf, B. & Hedrich, R. (1995) *Planta* **197,** 655–671.
18. Hamill, O. P., Marty, A., Neher, E., Sakmann, B. & Sigworth, F. J. (1981) *Pflügers Arch.* **391,** 85–100.
19. Wang, X. & Iino, M. (1997) *Plant Physiol.* **114,** 1009–1020.
20. Neher, E. (1992) *Methods Enzymol.* **207,** 123–131.
21. Edlund, A., Eklöf, S., Sundberg, B., Moritz, T. & Sandberg, G. (1995) *Plant Physiol.* **108,** 1043–1047.
22. Sentenac, H., Bonneaud, N., Minet, M., Lacroute, F., Salmon, J. M., Gaymard, F. & Grignon, C. (1992) *Science* **256,** 663–665.
23. Ketchum, K. A. & Slayman, C. W. (1996) *FEBS Lett.* **378,** 19–26.
24. Marten, I., Hoth, S., Deeken, R., Ache, P., Ketchum, K. A., Hoshi, T. & Hedrich, R. (1999) *Proc. Natl. Acad. Sci. USA* **96,** 7581–7586.
25. Hoth, S., Dreyer, I. & Hedrich, R. (1997) *J. Exp. Bot.* **48,** 415–420.
26. Daram, P., Urbach, S., Gaymard, F., Sentenac, H. & Cherel, I. (1997) *EMBO J.* **16,** 3455–3463.
27. Brüggemann, L., Dietrich, P., Dreyer, I. & Hedrich, R. (1999) *Planta* **207,** 370–376.
28. Abel, S. & Theologis, A. (1996) *Plant Physiol.* **111,** 9–17.
29. Iino, M., Tarui, Y. & Uematsu, C. (1996) *Plant Cell Environ.* **19,** 1160–1168.
30. Vanderhoef, L. N. & Dute, R. R. (1981) *Plant Physiol.* **67,** 146–149.
31. Hoth, S., Dreyer, I., Dietrich, P., Becker, D., Müller-Röber, B. & Hedrich, R. (1997) *Proc. Natl. Acad. Sci. USA* **94,** 4806–4810.
32. Bennett, M. J., Marchant, A., Green, H. G., May, S. T., Ward, S. P., Millner, P. A., Walker, A. R., Schulz, B. & Feldmann, K. A. (1996) *Science* **273,** 948–950.
33. Marchant, A., Kargul, J., May, S. T., Muller, P., Delbarre, A., Perrot-Rechenmann, C. & Bennett, M. (1999) *EMBO J.* **18,** 2066–2073.
34. Gälweiler, L., Guan, C., Iller, M., Wisman, E., Mendgen, K., Yephremov, A. & Palme, K. (1998) *Science* **282,** 2226–2230.
35. Müller, A., Guan, C., Gälweiler, L., Tanzler, P., Huijser, P., Marchant, A., Parry, G., Bennett, M., Wisman, E. & Palme, K. (1998) *EMBO J.* **17,** 6903–6911.

PLANT BIOLOGY